Applied Geochemistry 25 (2010) 684–695

Contents lists available at ScienceDirect

Applied Geochemistry

journal homepage: www.elsevier.com/locate/apgeochem

# Primary sink and source of geogenic arsenic in sedimentary aquifers in the southern Choushui River alluvial fan, Taiwan

Kuang-Liang Lu [a], Chen-Wuing Liu [a,*], Sheng-Wei Wang [a], Cheng-Shin Jang [b], Kao-Hung Lin [c], Vivian Hsiu-Chuan Liao [a], Chung-Min Liao [a], Fi-John Chang [a]

[a] Department of Bioenvironmental Systems Engineering, National Taiwan University, Taipei 106, Taiwan, ROC
[b] Department of Leisure and Recreation Management, Kainan University, Taoyuan 338, Taiwan, ROC
[c] Sustainable Environment Research Center, National Chen Kung University, Tainan 701, Taiwan, ROC

ARTICLE INFO

*Article history:*
Received 11 January 2009
Accepted 1 February 2010
Available online 8 February 2010

Editorial handling by D. Polya

ABSTRACT

This work characterized the sink and source/mobility of As in the As-affected sedimentary aquifers of the southern Choushui River alluvial fan, central Taiwan. Major mineral phases and chemical components were determined by XRD and X-ray photoelectron spectroscopy (XPS). The partitioning of As and Fe among cores were determined by sequential extraction. Based on XPS results, the primary forms of Fe were hematite, goethite and magnetite. Sequential extraction data and the XRF analysis indicated that Fe oxyhydroxides and sulfides were likely to be the major sinks of As, particularly in the distal-fan. Furthermore, Fe oxyhydroxides retained higher As contents than As-bearing sulfides. The reductive dissolution of Fe oxyhydroxides, which accompanied high levels of $HCO_3^-$ and $NH_4^+$ concentrations, was likely the principal release mechanism of As into groundwater in this area. The dual roles of Fe oxyhydroxides which are governed by the local redox condition act as a sink and source in the aquifer. Ionic replacement by $PO_4^{3-}$ and $HCO_3^-$ along with seasonal water table fluctuation, caused by monsoons and excessive pumping, contributed specific parts of As in the groundwater. The findings can be used to account for the inconsistency between Fe and As concentrations observed in groundwater.



## 1. Introduction

Arsenic is abundant in the earth's crust. It undergoes numerous complex transformations, such as oxidation–reduction, precipitation–dissolution, adsorption–desorption and biochemical methylation. Arsenic causes serious environmental problems in several parts of the world, including Bangladesh, India, Nepal, Thailand, China, Taiwan, Vietnam, Chile, Hungary and parts of the USA (Smedley and Kinniburgh, 2002; McArthur et al., 2004; Hossain, 2006; Bhattacharya et al., 2007). It has been shown to be a major risk factor for blackfoot disease (BFD), which was first identified in the Chianan Plain, Taiwan (Chen et al., 1994).

In Taiwan, BFD was an endemic disease due consumption of high As waters abstracted from deep wells (70–200 m) in the Chianan Plain (Tseng, 1977). Before 1997, according to statistical data, there were 2758 patients suffering from BFD in Taiwan. Groundwater from shallow wells (20–70 m) in the southern region of the Choushui River alluvial fan, adjacent to the Chianan Plain, was also enriched with As (Guo et al., 1994). The As content of the water in around 70% of the wells in the Choushui River alluvial fan exceeded the drinking water standard in Taiwan (0.01 mg $L^{-1}$) (Taiwan Sugar Company, 1999, 2000, 2003, 2006). Such high As concentrations in groundwater were postulated to originate from the aquitards with geological ages which are between 3 and 9 ka or from the Holocene transgression in the area of the Chianan Plain (Liu et al., 2006).

Generally, the mobilization of As within sediments depends on mineral phases in aquifers and aquitards (Anawar et al., 2003), and the redox conditions of groundwater (Zheng et al., 2004). Three pathways which could be responsible for high As concentration in the groundwater were posited, including: (1) oxidation of As-bearing sulfides; (2) reductive dissolution of As-bearing Fe and/or Mn oxyhydroxides; and (3) competitive exchange reaction of ions, such as $PO_4^{3-}$, $CO_3^{2-}$ and organic C. Currently, the reductive dissolution of As-bearing Fe and/or Mn oxyhydroxides with the concurrent release of Fe, As and $HCO_3^-$, is regarded as the most likely mechanism that is responsible for high levels of As under anaerobic conditions (Nickson et al., 1998, 2000, 2005; McArthur et al., 2001). However, dissolved As exhibited low correlation with Fe (Anawar et al., 2003). Therefore, competitive and complexation reactions, biomineralization and re-adsorption have also been thought to accompany the onset of reductive dissolution, whether mediated by

* Corresponding author. Fax: +886 2 2363 9557.
*E-mail address:* lcw@gwater.agec.ntu.edu.tw (C.-W. Liu).

0883-2927/$ - see front matter © 2010 Elsevier Ltd. All rights reserved.
doi:10.1016/j.apgeochem.2010.02.001

microbial or geochemical processes (Appelo et al., 2002; Islam et al., 2005; Kocar et al., 2006, 2008).

Although the content and the mobility of As within the subsurface in the southern Choushui River alluvial fan has been postulated to be related to local lithology and reductive conditions, respectively (Liu et al., 2006; Wang et al., 2007), no evidence has as yet clarified the partitioning and interaction of As with geological sediments. Therefore, this study aimed to differentiate the dominant sink/source of As, particularly within the interval of the well screen, by using sequential extraction approaches, and spectroscopic and microscopic methods. The geochemical conditions of groundwater in the corresponding wells were also examined. Data were incorporated to understand the partitioning and release mechanisms of As in this area.

## 2. Study area and analytical methods

### 2.1. Site description and sediment collection

The Choushui River alluvial fan in Taiwan encompasses Chang-Hwa and Yun-Lin Counties. Yun-Lin County is located in the southern part of the Choushui River alluvial fan, and is bordered by the Taiwan Strait to the west, the Central Mountain to the east, the Choushui River to the north, and the Peikang River to the south (Fig. 1a). The Choushui River alluvial fan was formed in the Late Quaternary period and is partitioned into proximal-, mid- and distal-fan areas (Central Geological Survey, 1999). Based on subsurface hydrogeological analysis to a depth of around 300 m, the formation is divided into six inter-layered sequences, including

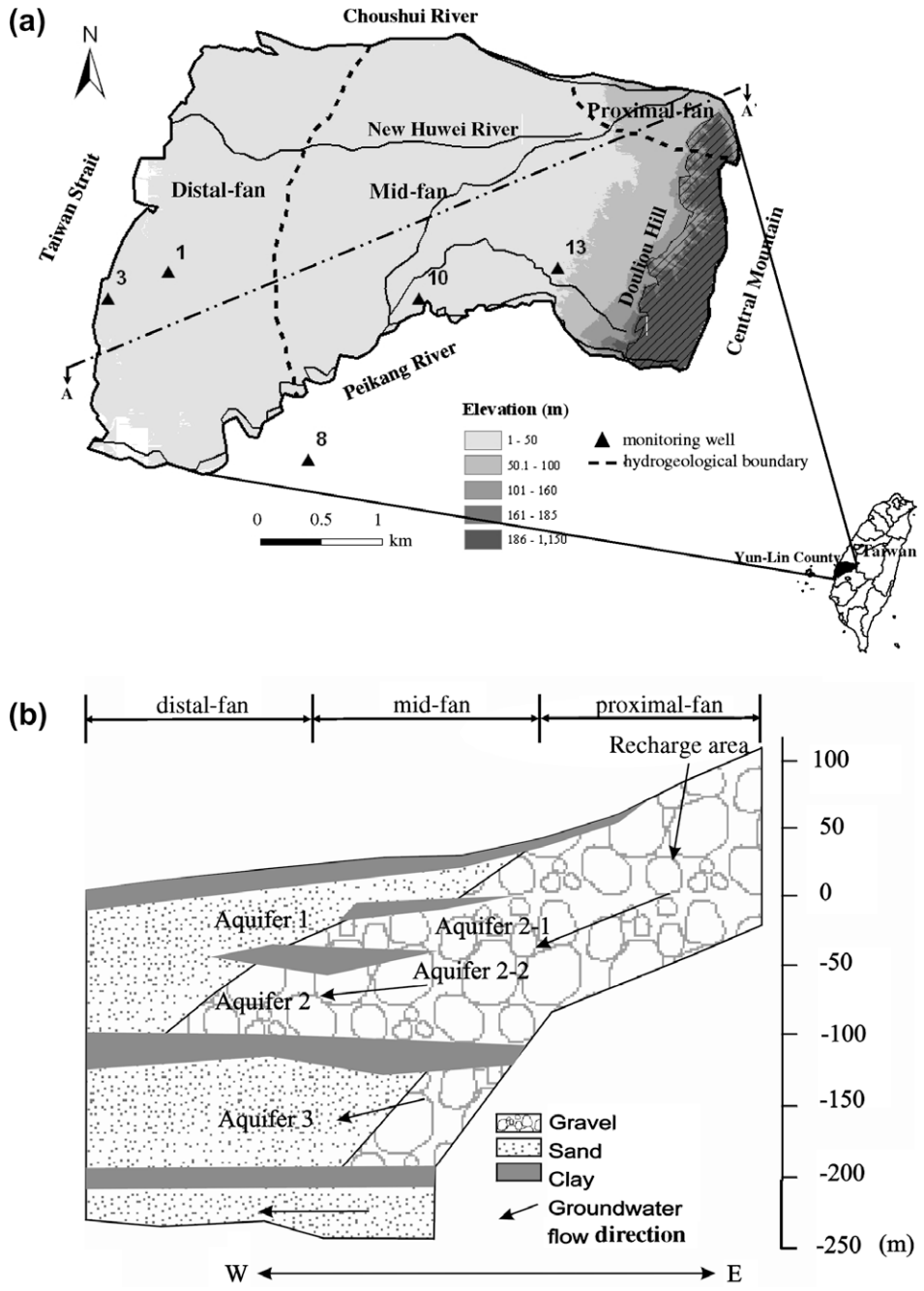


**Fig. 1.** (a) Location of the five drilling stations in Yun-Lin County and (b) the hydrogeological profile (along line AA′ in (a) in the study area.

three marine sequences and three non-marine sequences, in the distal- and mid-fan areas. The non-marine sequences of the formation, with coarse sediment, ranging from medium sand to highly permeable gravel, are typically classified as aquifers, whereas the marine sequences of the formation with fine sediments can be regarded as aquitards. The hydrogeological formation of the proximal-fan, which consists entirely of gravel and sand, is considered to be an unconfined aquifer and an important groundwater recharge area (Fig. 1b). More relevant information can be found in Liu et al. (2006).

Five boreholes in the southern part of Yun-Lin County were selected for the investigation of field geochemistry (Fig. 1a). Stations 1 and 3 were located in the distal-fan, whereas Stations 8, 10 and 13 were located in the mid-fan. Thirty-four samples, from the Core Laboratory of the Central Geological Survey, which had been preserved, were collected for analysis (Table 1).

### 2.2. Analytical methods

#### 2.2.1. Aqueous phase

Groundwater quality data were obtained from the annual survey of the Taiwan Sugar Company (1999, 2000, 2003, 2006). Additionally, groundwater samples for the same six depth-specific wells were collected and analysed in July, 2009. Time-averaged values of physicochemical parameters of groundwater samples were used. The field sampling methods adopted followed the NIEA code W103.50B set by the Taiwan Environment Protection Agency. At least three wellbore volumes of groundwater were pumped before sampling. Dissolved $O_2$ (DO), temperature, pH, electrical conductivity (EC) and $E_H$ were measured in a flow-through cell every 5 min during well purging. Cell sensors were calibrated with standard solutions (all from Merck), which have pH = 4.0, 7.0 and 10.0; EC = 1410 μS $cm^{-1}$; $E_H$ = 280 mV, in the field before measuring any of these parameters (APHA, 1998). Water samples were collected only after pH and EC had stabilized, and the fluctuations of pH and relative EC were less than 0.1% and 5%, respectively. After purging, a probe (MiniSonde manufactured by HydroLab, USA), which is 5 cm in diameter and 70 cm in length, and is inclusive of a data logger, a circulator and three sensors for temperature, EC, pH, $E_H$ and DO measurements, was lowered down to the screen position of the well casing and remained there for at least 10 min before water quality parameters were recorded (Chen and Liu, 2003).

Water samples for trace metal and other cation determinations were filtered through 0.45 μm glass fiber papers and acidified with $HNO_3$ (Merck ultrapure grade) to pH 2. To avoid trapping or dissolving atmospheric $O_2$, a rubber tube was extended from the pump line to the bottom of the bottle. After 2 or 3 bottle volumes of water flowed out, the bottle was tightly stoppered so eliminating air bubbles. Samples were then kept in ice boxes and delivered to the laboratory within 24 h. Dissolved organic C (DOC) was measured using a high temperature combustion method. The anions $NO_3^-$ and $SO_4^{2-}$ were determined by spectrophotometry using the Cd reduction and turbidimetric methods, respectively (APHA, 1998). Dissolved $PO_4^{3-}$ was determined by spectrophotometry with ammonium molybdate and stannous chloride to form a blue complex. Trace metal ions including Fe were measured by atomic absorption spectroscopy (AAS). A total of 15 samples including blank, spike, duplicate and check samples (standard solutions from Merck) were measured sequentially (APHA, 1998). For Fe, the detection limit was 0.05 mg $L^{-1}$; variance of duplicate measurements were less than 3%; recoveries of check and spike samples were between 90% and 110%.

#### 2.2.2. Solid phase

Freeze-dried and sieved samples were used in the analyses to ensure representative sampling. A high-resolution X-ray photoelectron spectrometer (HR-XPS) (PHI Quantera SXM), which was equipped with a Kα X-ray beam at 3.8 kW generated from an Al rotating anode, was used to characterize the surface. Each spectrum was obtained by plotting the measured photoelectron intensity as a function of the binding energy. Binding energies of photoelectrons were calibrated with reference to the aliphatic adventitious hydrocarbon C (1s) peak at 284.6 eV. The elemental compositions of mineral grains were determined by scanning electron microscopy (SEM) and energy dispersive spectroscopy (EDS) using a S-3000 N instrument (Hitachi). The amounts of the various elements (Si, Al, Fe, Ca, K, Mn, etc.) in the core samples were determined by X-ray fluorescence (XRF) (Spectro, XEPOS). The constituent minerals of the sediments were identified by X-ray diffractometry (XRD) (Bruker, D8). Percentage abundance of total C was determined with a model 2400 CHN analyzer (VarioEL-III, Heraeus, Germany). Total organic C (TOC) contents were then determined by subtracting the amount of C present as carbonate from the total amount of C present.

Sequential extraction using freeze-dried sediments was conducted to determine As and Fe contents in the operationally defined mineral phases. The extraction procedure was based on those of Keon et al. (2001). In total, 40 mL of each extractant was added to 1.0 g dried sediment in a 50 mL centrifuge tube. Suspen-

**Table 1**
Lithology, corresponding hydrogeological sequence and total organic C of core samples.

| Site location-depth (m) | Lithology | Hydrogeological sequence | Total organic C (%) |
|---|---|---|---|
| 1–6 | Silty sand | Surfacial layer | 0.20 |
| 1–30 | Silty sand | Aquifer 1 | 0.20 |
| 1–36 | Silty sand | Aquifer 1 | 0.36 |
| 1–42 | Silty sand | Aquifer 1 | 0.40 |
| 1–48 | Silty sand | Aquifer 1 | 0.46 |
| 1–54 | Grey mud | Aquitard 2 | 0.20 |
| 3–31 | Clay | Aquitard 1 | 0.33 |
| 3–36 | Silty sand | Aquifer 1 | 0.32 |
| 3–42 | Silty sand | Aquifer 1 | 0.37 |
| 3–49 | Silty sand | Aquifer 1 | 0.12 |
| 3–51 | Clay | Aquifer 1 | nm |
| 3–55 | Silty sand | Aquifer 1 | 0.10 |
| 3–162 | Clay | Aquitard 2 | nm |
| 8–130 | Grey clay | Aquitard 2 | nm |
| 10–6 | Clay | Surfacial layer | 0.31 |
| 10–10 | Silty sand | Aquifer 1 | 0.92 |
| 10–16 | Gravel sand | Aquifer 1 | 1.32 |
| 10–22 | Clay | Aquifer 1 | 0.28 |
| 10–25 | Clay | Aquifer 1 | 0.17 |
| 10–39 | Grey mud | Aquitard 2 | 0.18 |
| 10–51 | Clay | Aquitard 2 | 0.16 |
| 10–55 | Silty sand | Aquifer 2 | 0.24 |
| 10–58 | Silty sand | Aquifer 2 | 0.07 |
| 10–61 | Gravel sand | Aquifer 2 | 0.37 |
| 10–152 | Grey mud | Aquitard 3 | nm |
| 13–12 | Silty sand | Aquifer 1 | 0.19 |
| 13–15 | Gravel sand | Aquifer 1 | 0.30 |
| 13–21 | Gravel sand | Aquifer 1 | 0.30 |
| 13–27 | Gravel sand | Aquifer 1 | 0.23 |
| 13–39 | Clay | Aquitard 1 | 0.25 |
| 13–75 | Clay | Aquifer 2 | 0.20 |
| 13–78 | Gravel | Aquifer 2 | 0.20 |
| 13–84 | Gravel sand | Aquifer 2 | 0.36 |
| 13–90 | Gravel sand | Aquifer 2 | 0.40 |

nm = not measured.

sions were shaken for a specified time and the supernatant was decanted. These procedures target weakly adsorbed As (1 mol $L^{-1}$ $MgCl_2$, pH 8; MG step), strongly adsorbed As (1 mol $L^{-1}$ $NaH_2PO_4$, pH 4–5; PHOS step), As coprecipitated with carbonates, acid volatile sulfides, amorphous metal oxides and magnetite (1 mol $L^{-1}$ HCl followed by 0.2 mol $L^{-1}$ oxalic acid, pH 3; HCl and OX steps), As coprecipitated with crystalline Fe oxides and amorphous sulfides (0.5 mol $L^{-1}$ titanium chloride–sodium citrate–tetrasodium EDTA-bicarbonate, pH 7; TiCEB step), As coprecipitated with silicate minerals or $As_2O_3$ (10 mol $L^{-1}$ HF; HF step), and As incorporated in pyritic phases (concentrated $HNO_3$; NIT step). A final hot concentrated $HNO_3$ and $H_2O_2$ digest (following EPA 3050B) of the residue targets As incorporated in crystalline sulfides such as orpiment, and other recalcitrant phases (HOT NIT step) (USEPA, 1997). These extraction steps are referred to hereafter as MG, PHOS, HCl, OX, TiCEB, HF, NIT, and HOT NIT, respectively, as classified by Swartz et al. (2004).

To determine the total concentrations of As, samples were digested with 30% $H_2O_2$ and 9.6 M HCl, and for Fe were digested with hot concentrated $HNO_3$ and $H_2O_2$ following EPA 3050B. After filtering, total As concentrations of each extract were determined by using an electro-thermal atomic absorption spectrometer (AAS, Perkin-Elmer AA100) and a hydride generation (HG) system (Perkin-Elmer FIAS100). To reduce As to arsine, 0.5% $NaBH_4$ in 0.25% NaOH and 1 M HCl were added. Total Fe was determined using flame atomic absorption spectrometry (AAS, Perkin-Elmer AA100).

## 3. Results

### 3.1. Geochemistry of groundwater

Table 2 summarizes the information on aqueous parameters, locations and screen ranges of these wells. In these wells, reducing conditions were evidenced by negative $E_H$, meanwhile the sampled groundwaters were mildly alkaline (pH > 7) exclusive of W13. Electrical conductivity typically increased from mid-fan to distal-fan, and decreased with increasing depth from aquifer 1 to aquifer 2 (Table 2). Selected groundwater samples were characterized as Na–Ca–$HCO_3$ and Ca–Na–$HCO_3$ types with $HCO_3^-$ and $Cl^-$ as the dominant anions, though another type was also observed in W13-1 (Ca–Mg–$HCO_3$) (Table 2). Except for W13-2, most of the dissolved N was present as $NH_4$, indicating the onset of a reducing environment. Dissolved As and organic C in groundwater ranged from 0.01 to 0.50 mg $L^{-1}$ and 0.7 to 3.6 mg $L^{-1}$, respectively. Lowest levels of As and DOC concentrations were observed concurrently in W13. Most of the dissolved S occurred as $SO_4^{2-}$, with the highest and the lowest concentrations in different aquifers of W10. The $PO_4^{3-}$ concentrations ranged from 0.2 to 37.0 mg $L^{-1}$ with the highest value in W1-1 (Table 2). Dissolved Fe and Mn concentrations exhibited similar variations with depth or the composition of the deposits. Furthermore, $HS^-$ and $CH_4$ were not detected in these wells.

### 3.2. Sediment characteristics and distribution of elements

Core samples obtained from both aquifers and aquitards in the southern Choushui River alluvial fan consisted of silty sand, organic-rich mud and clay as shown in Table 1. In addition, TOC contents ranged from 0.07% to 1.32% with a mean value of 0.32% (Table 1). Furthermore, the TOC contents were distributed evenly and showed no correlation with texture, location or As content. Illite and chlorite, which were identified as the major clay minerals by XRD, were crystalline, showing mild weathering (Liu, 1999).

Each XPS result for Fe (Fig. 2) comprises two curves – (1) the experimental curve after smoothing and (2) the curve of the fitted components. The Fe signal is a doublet because of spin coupling, corresponding to $Fe2p_{3/2}$ (BE = 706–718 eV) and $Fe2p_{1/2}$ (BE = 723–732 eV). The fitted results (Fig. 2) indicate that the $Fe2p_{3/2}$ line can be fitted by two components with binding energies of about 711 and 714 eV, respectively. The primary peak ($Fe2p_{3/2}$) at 710.6–710.8 eV is characteristic of Fe(III) in $Fe_2O_3$ compounds (Fig. 2a–c); that at 711.4–711.8 eV is characteristic of Fe(III) in FeOOH compounds (Fig. 2d–g), and that at 708.2–710.4 eV is characteristic of mixed-valence Fe in $Fe_3O_4$ compounds (Fig. 2h). In the distal-fan, hematite and goethite dominate in aquifers and aquitards, respectively. In the mid-fan, the Fe mineral distributions are complex. The detection limit is such that the spectra of $Mn2p_{3/2}$ and $As3d_{5/2}$ yielded no information regarding the specific mineral compounds of Mn and As.

Samples 1–6, 1–54, 3–51 and 3–162 were chosen for further investigation by SEM–EDS. Pyrite was found in both samples 1–6 and 1–54 (Fig. 3a and b) and was similar to that in the Bangladesh

**Table 2**
Physicochemical parameters of groundwater samples of six depth-specific wells in the study area.

| Measurement | Well location-aquifer Screen range (m) | | | | | |
|---|---|---|---|---|---|---|
| | W1-1[a] (36–48) | W3-1 (36–60) | W10-1 (10–28) | W10-2 (55–64) | W13-1 (14–32) | W13-2 (78–96) |
| $E_H$ (mV)[b] | −170.3 ± 54.1 | −154.3 ± 52.3 | −93.0 ± 50.8 | −115.8 ± 69.0 | −101.3 ± 34.4 | −37.5 ± 35.3 |
| EC (μs $cm^{-1}$)[b] | 981.9 ± 86.1 | 1985.7 ± 880.0 | 1272.1 ± 375.6 | 708.8 ± 357.2 | 499.0 ± 80.9 | 354.0 ± 27.2 |
| pH[b] | 7.7 ± 0.2 | 7.6 ± 0.4 | 7.1 ± 0.1 | 7.3 ± 0.3 | 6.9 ± 0.2 | 6.6 ± 0.3 |
| $Ca^{2+}$ (mg $L^{-1}$)[c] | 44.6 ± 5.7 | 105.9 ± 24.5 | 153.3 ± 16.4 | 60.8 ± 29.1 | 65.9 ± 5.8 | 40.1 ± 3.7 |
| $Mg^{2+}$ (mg $L^{-1}$)[c] | 34.2 ± 3.7 | 73.4 ± 32.8 | 55.1 ± 14.3 | 26.1 ± 12.7 | 17.1 ± 4.6 | 11.3 ± 1.6 |
| $Na^+$ (mg $L^{-1}$)[d] | 129.7 ± 28.3 | 323.3 ± 131.9 | 105.7 ± 8.2 | 62.7 ± 22.2 | 17.0 ± 1.5 | 19.7 ± 1.0 |
| $K^+$ (mg $L^{-1}$)[d] | 21.9 ± 2.2 | 29.0 ± 18.7 | 3.9 ± 1.8 | 12.8 ± 5.6 | 1.0 ± 0.2 | 1.4 ± 0.8 |
| $NH_4^+$ (mg $L^{-1}$)[b] | 4.6 ± 2.9 | 6.5 ± 5.8 | 2.7 ± 0.8 | 6.5 ± 1.5 | 1.4 ± 0.4 | 0.1 ± 0.2 |
| DOC (mg $L^{-1}$)[d] | 3.1 ± 1.0 | 3.3 ± 1.1 | 2.9 ± 1.3 | 3.6 ± 0.4 | 1.3 ± 0.9 | 0.7 ± 0.8 |
| $HCO_3^-$ (mg $L^{-1}$)[c] | 394.4 ± 90.6 | 392.8 ± 36.8 | 375.3 ± 32.4 | 375.3 ± 86.4 | 186.0 ± 13.4 | 106.9 ± 12.4 |
| $Cl^-$ (mg $L^{-1}$)[d] | 64.1 ± 64.4 | 350.9 ± 406.3 | 87.7 ± 75.3 | 20.4 ± 14.5 | 7.1 ± 6.4 | 6.4 ± 5.8 |
| $NO_3^-$ (mg $L^{-1}$)[c] | 0.1 ± 0.0 | 0.1 ± 0.1 | 0.1 ± 0.1 | 0.1 ± 0.1 | 0.3 ± 0.4 | 2.6 ± 1.8 |
| $SO_4^{2-}$ (mg $L^{-1}$)[d] | 72.5 ± 28.4 | 67.3 ± 49.5 | 264.0 ± 72.9 | 13.0 ± 13.7 | 58.0 ± 42.8 | 73.0 ± 27.8 |
| $PO_4$ (mg $L^{-1}$)[e] | 37.0 ± 3.8 | 1.5 ± 2.0 | 0.8 ± 0.8 | 2.2 ± 1.8 | 0.6 ± 0.6 | 0.2 ± 0.1 |
| As (mg $L^{-1}$)[b] | 0.50 ± 0.18 | 0.25 ± 0.18 | 0.23 ± 0.09 | 0.29 ± 0.23 | 0.02 ± 0.02 | 0.01 ± 0.01 |
| Fe (mg $L^{-1}$)[b] | 1.2 ± 0.6 | 4.4 ± 2.9 | 8.1 ± 2.4 | 18.6 ± 35.3 | 17.6 ± 3.0 | 0.3 ± 0.4 |
| Mn (mg $L^{-1}$)[b] | 0.2 ± 0.0 | 0.6 ± 0.2 | 0.2 ± 0.1 | 0.5 ± 0.3 | 0.8 ± 0.2 | 0.0 ± 0.0 |

[a] First and second numbers denote corresponding location and aquifer, respectively.
[b,c,d] Average ± 1 standard deviation of 5-, 4- and 3-year data, respectively.
[e] Only data from 2009.

studies, where it was identified as the framboidal-diagenetic type (Nickson et al., 2000; Akai et al., 2004). In addition, gibbsite ($Al(OH)_3$), a secondary mineral and one of the major Al minerals, was present in the clay sample 1–6 (Klein and Hurlbut, 1999) (Fig. 3c). The oxidation of pyrite was evidenced by the EDS data, and was associated with the wet conditions (Nickson et al., 2000) (Fig. 3d). No well characterized Fe or S minerals were observed in samples 3–51 and 3–162. Although the four samples were all collected from the distal part of the southern Choushui River alluvial fan, the redox conditions and minerals in the sequence exhibited distinct characteristics.

More than 95 wt.% of the core samples, as determined by the XRF analysis, was comprised of Si, Al, Fe and K (Table 3). These results were similar to those identified in Bangladesh (Anawar et al., 2003; Swartz et al., 2004). Sulfur and Ca, which represented around 2 wt.% of the core samples, were the minor constituent elements. Samples 1–6 and 3–51 had the highest As and Mn concentrations, respectively. Data from the core samples revealed that the Fe and S contents in the sediments were closely correlated with those of As ($r^2 = 0.49$, $p = 0.05$; $r^2 = 0.86$, $p < 0.05$), as confirmed by regression analysis, there was also a close correlation between Fe and S ($r^2 = 0.62$, $p < 0.05$) (Fig. 4). Hence, these relationships showed that As in the sediments was associated with Fe oxyhydroxides and As-bearing sulfides, as described by Anawar et al. (2003) in Bangladesh.

### 3.3. Partitioning of As and Fe

Data from sequential extractions revealed that the contents of operationally defined fractions of solid phase As covaried with location and lithology, and the content range for either pool typically spanned less than one order of magnitude. Details of the analyses of the extraction results for As and Fe are presented in Figs. 5–8. Arsenic in the MG extraction was generally non-detectable. Contents of solid phase As leached by PHOS, HCl and NIT + HOT NIT extractants accounted for most of the extractable As, although the HF extractant was not measured (Figs. 5 and 6). Typically, the HCl extractant contained higher As contents than the others, indicating the As-hosting capacity of amorphous Fe oxyhydroxides. In addition, the NIT + HOT NIT extractants accounted for significant portions of the As in the sediments collected from the distal-fan. The sum of the As extracted from the HCl, OX and TiCEB extractants exceeded that extracted in the NIT + HOT NIT extractants, revealing that Fe oxyhydroxides contained more As than As-bearing sulfides in this area (Fig. 6). The partitioning of As in the distal-fan distributed evenly over the PHOS, HCl, OX, TiCEB and NIT + HOT NIT pools, but was concentrated in the PHOS, HCl and OX pools in the mid-fan (Figs. 5 and 6). Lithologically, the clay samples contained more As than that the sandy samples, as stated by Liu et al. (2006). Solid As contents were typically higher in the distal-fan than in the mid-

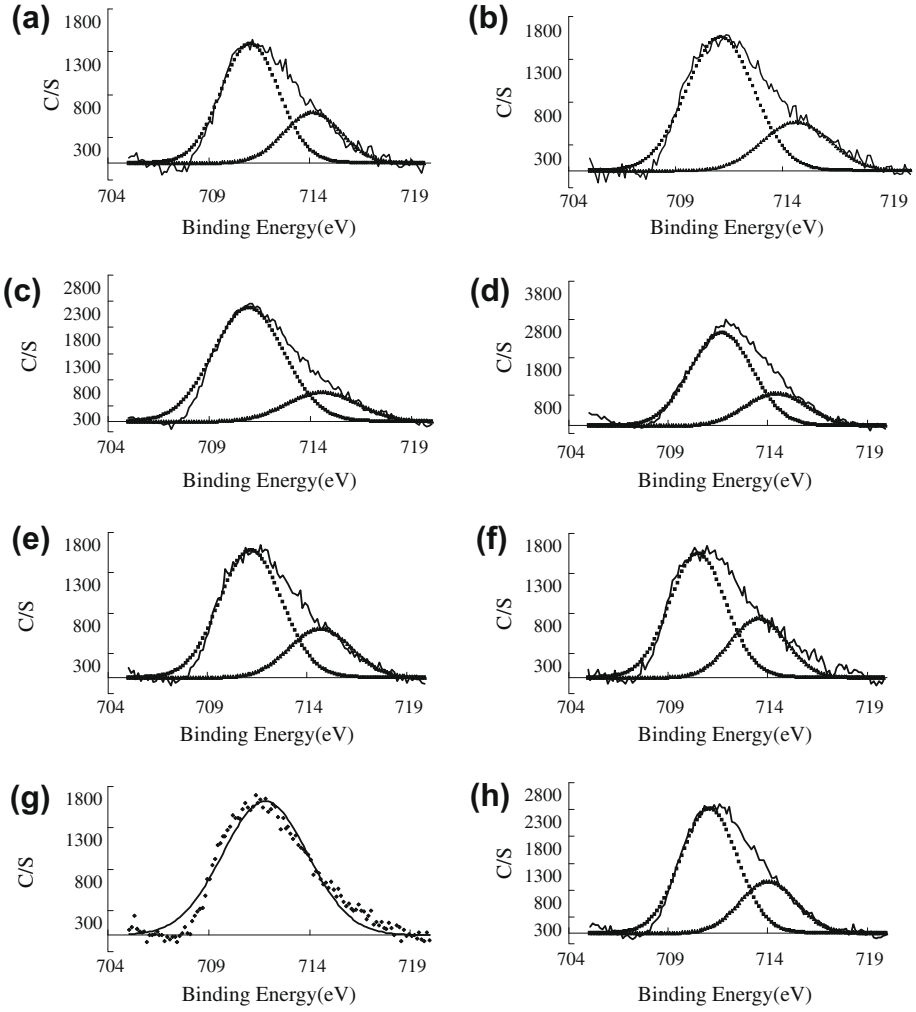


**Fig. 2.** Curve fitting data of the $Fe2p_{3/2}$ core level. (a) 1–6, (b) 3–51, (c) 8–130, (d) 1–54, (e) 3–162, (f) 10–152, (g) 13–39 and (h) 10–39. The solid line represents the experimental curve after smoothing and the dotted lines represent the fitted curve.

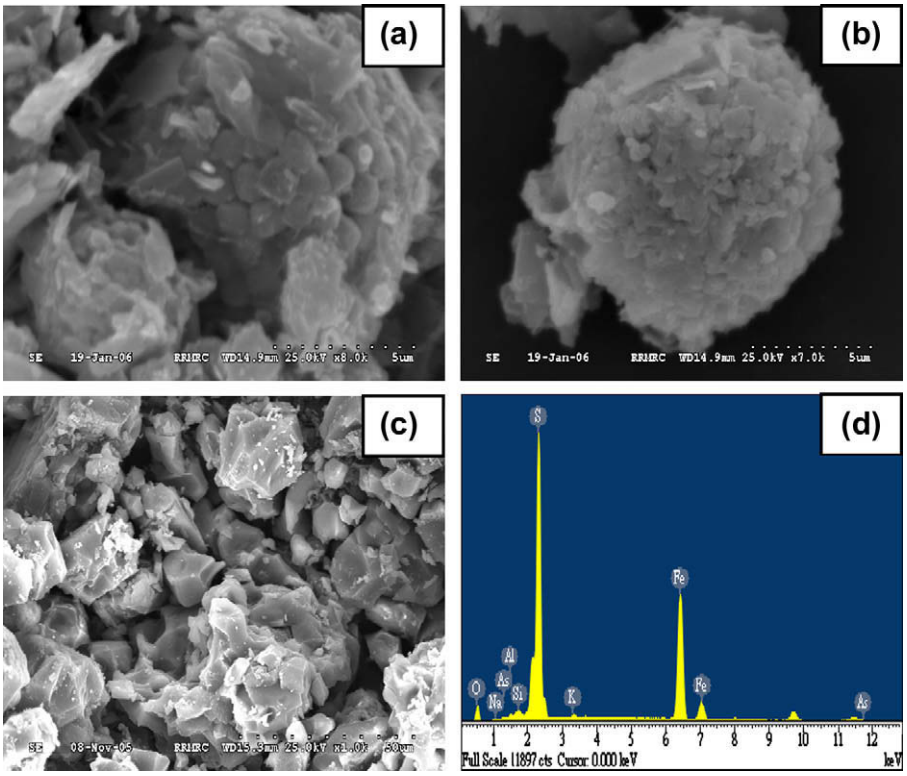


**Fig. 3.** Scanning electron microscope analysis of samples 1–6 and 1–54. (a and b) Framboidal early-diagenetic pyrite in samples 1–6 and 1–54, respectively, (c) the aggregation of gibbsite ($Al(OH)_3$) in sample 1–6, and (d) EDS data of sample 1–54.

**Table 3**
Major elements (wt.%), As and Mn (mg $kg^{-1}$) contents of core samples.

| Measurement | Site location-depth (m) | | | | | | | |
|---|---|---|---|---|---|---|---|---|
| | 1–6 | 1–54 | 3–51 | 3–162 | 8–130 | 10–39 | 10–152 | 13–39 |
| Si | 62.2 | 66.4 | 64.9 | 70.4 | 62.6 | 60.4 | 65.1 | 71.4 |
| Al | 25.9 | 25.6 | 25.1 | 23.8 | 29.5 | 30.5 | 26.2 | 22.5 |
| Fe | 5.3 | 3.8 | 3.9 | 3.0 | 3.7 | 3.9 | 4.1 | 2.6 |
| K | 2.9 | 3.1 | 2.8 | 2.6 | 3.5 | 3.6 | 3.2 | 2.8 |
| S | 1.7 | 0.7 | 0.6 | 0.0 | 0.2 | 0.0 | 0.1 | 0.1 |
| Ca | 1.8 | 0.4 | 2.6 | 0.3 | 0.3 | 1.5 | 1.3 | 0.7 |
| Total | 99.8 | 100.1 | 99.9 | 100.1 | 99.8 | 99.9 | 100 | 100.1 |
| As | 130.9 | 104.2 | 49.2 | 28.1 | 34.3 | 18.6 | 27.1 | 20.5 |
| Mn | 431.4 | 51.0 | 928.2 | 65.6 | 311.8 | 578.4 | 368.8 | 724.0 |

fan, and more concentrated in the clay and/or muddy samples than in the sandy and/or gravel samples.

Lithologically, the extraction data for Fe distributed similarly to those of As, which were described above (Figs. 7 and 8). The total Fe contents ranged from 32,000 to 54,000 mg $kg^{-1}$ in the cores. The MG and PHOS extracts accounted for only small portions of the Fe contents. Most of the Fe, approximately 80%, was concentrated in the HCl and HF extracts (Fig. 8). The Fe contents in the distal-fan were higher than that in the mid-fan, and distributed heterogeneously within the screen interval areas (Figs. 7 and 8). Hence, despite the presence of Fe-silicate minerals within the HF pool, non-crystalline oxyhydroxides contained the dominant portions of Fe as found by sequential extraction (Keon et al., 2001).

## 4. Discussion

### 4.1. Primary sinks of arsenic

From the XPS data, Fe minerals were characterized as oxyhydroxides comprising hematite, goethite and magnetite. Iron oxides are a major source of labile As as they commonly have large surface areas, and a high capacity and strong affinity for sorbing As. Numerous studies have also suggested the adsorption of As on Fe (oxy)hydroxides (Lenoble et al., 2002; Sherman and Randall, 2003). The relationships and partitioning of As with Fe and S in the solid phase were confirmed by both XRF and sequential extraction, indicating that the distribution of As was associated with Fe/S or Fe/S-rich phases in the southern part of the Choushui River alluvial fan. Further associations between As with both Fe and sulfide minerals were indicated by the extraction data. To eliminate the heterogeneity from the screen range, the cumulative As contents in the specific steps were considered. The total As contents leached by HCl, OX and TiCEB extracts in the range of the screen were well correlated with Fe contents in the same pools ($r^2 = 0.94$, $p < 0.05$; Fig. 9a). Subsequently, the amount of As in the NIT pool in all cores was also correlated closely with Fe contents in the same pool ($r^2 = 0.81$, $p < 0.05$; Fig. 9b). The HCl, OX and TiCEB extracts represent the major part of the Fe oxyhydroxides in the sediments and the NIT step the major pyritic phase. The distribution of As, particularly within the well screen area,

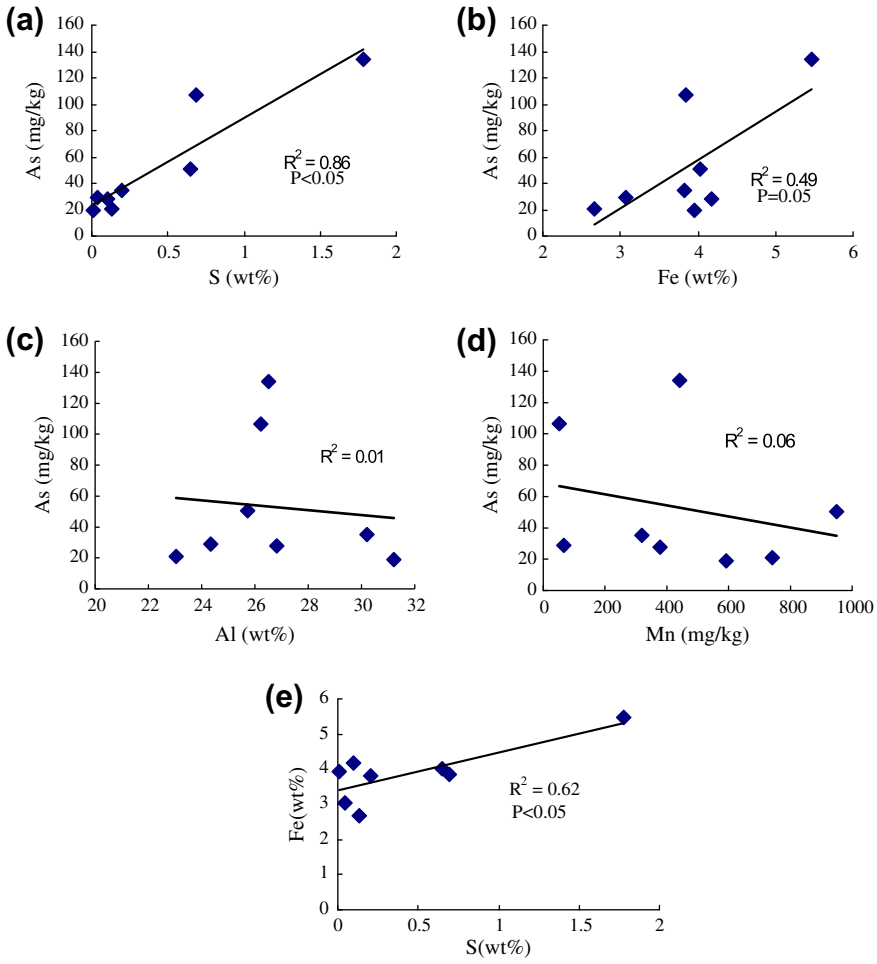


**Fig. 4.** Relationships of As content with (a) S; (b) Fe; (c) Al; (d) Mn among sediment cores. Relationship of Fe content with (e) S among sediment cores.

was related to Fe oxyhydroxides and As-bearing sulfides (i.e. pyrite) in this region.

The enrichment of As has been postulated to be associated with Fe oxyhydroxides and As-bearing sulfides in the Bangladesh As-enriched area (Smedley and Kinniburgh, 2002), as observed here. However, over-pumping of groundwater in the area has not only caused seawater intrusion but also supplied $O_2$, particularly in the distal-fan (Liu et al., 2003). Subsequently, the re-oxidation of $Fe^{2+}$ and the oxidation of sulfides (i.e. pyrite) could lead to the formation of amorphous Fe oxyhydroxides, which provided extra adsorption surface sites for the released As species. In addition, based on the SEM–EDS data, pyrite was identified as authigenic framboidal type, indicating the S reduction also occurred in the distal-fan area. The association between As and pyrite was confirmed by EDS data (Fig. 3d). Hence, Fe oxyhydroxides and As-bearing sulfides are the dominant As-contained solids in this area, especially in the distal-fan. Notably, compared to the amounts of Fe and S from the XRF data, Fe minerals were abundant within the well screen ranges in contrast to As-bearing sulfides. Aside from the role of dominant sink of As, Fe oxyhydroxides may also act as the principal source of As in reducing conditions.

### *4.2. Arsenic release due to the reductive dissolution of Fe oxides and ion interactions*

Groundwaters characterized as high pH with elevated concentrations of dissolved Fe, $HCO_3^-$, $NH_4^+$ and $PO_4^{3-}$, were similar to those observed in other As-rich aquifers with reducing conditions (Shimada, 1996; McArthur et al., 2001; Rowland et al., 2008). Additionally, aqueous As concentrations were strongly correlated with $HCO_3^-$ ($r^2 = 0.84$), $NH_4^+$ ($r^2 = 0.69$), DOC ($r^2 = 0.61$) and $E_H$ values ($r^2 = 0.71$) (Fig. 10), but poorly correlated with Fe ($r^2 = 0.21$) and $SO_4^{2-}$ ($r^2 < 0.01$). These general characteristics and relationships are consistent with the mechanism of reductive dissolution of Fe oxyhydroxides via microbial respiration, with concomitant release of associated adsorbed and/or coprecipitated As, which has also been found in Bangladesh and in other areas (Shimada, 1996; Harvey et al., 2002; Kocar et al., 2008; Rowland et al., 2008). Furthermore, due to the detection of authigenic framboidal pyrite within the well screen in Drilling Station 1 (Fig. 3b), it is suggested that formation of sulfides, rather than oxidative dissolution, is more likely in these deposits, and may also explain the low concentration of aqueous Fe in W1-1 (Table 2). Hence, the Fe oxyhydroxides played dual roles in this area and were governed by the local redox conditions. The presence of framboidal pyrite represents a minor sink of As under reducing conditions supplemented by $SO_4^{2-}$ from seawater intrusion.

Local groundwater quality revealed a lower ratio of Fe to $HCO_3^-$ than the 1:2 which has been calculated from other studies in the presence of reductive dissolution of Fe oxyhydroxides mediated by microbial action (Chapelle and Lovley, 1992; Lovley, 1997; Nealson, 1997; Banfield et al., 1998; Chapelle, 2000). Aside from degradation by microbial action, authigenic weathering also contributes to $HCO_3^-$ concentrations as well as $PO_4^{3-}$ (BGS and DPHE, 2001; McArthur et al., 2001; Bhattacharya et al., 2002; Nickson et al., 2005; Stollenwerk et al., 2007). Indeed, moderate to high cor-

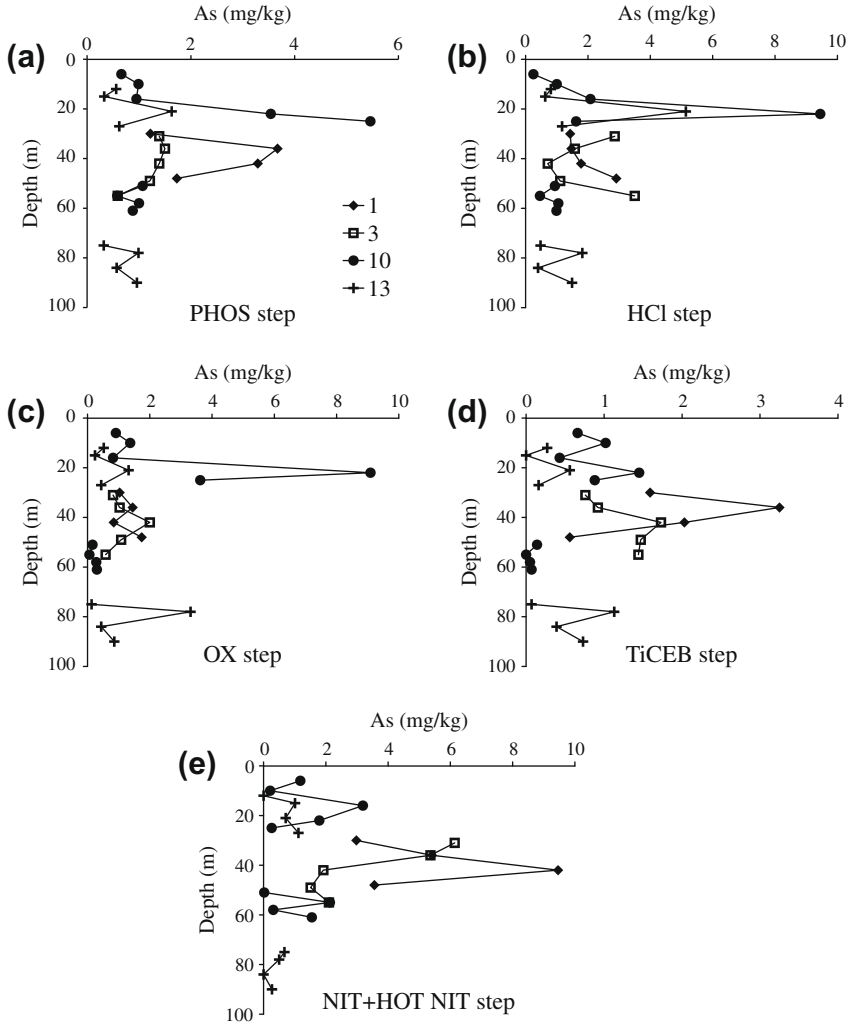


**Fig. 5.** Depth-variation profiles of As contents in (a) PHOS step, (b) HCl step, (c) OX step, (d) TiCEB, and (e) NIT + HOT NIT step. Diamond (♦), hollow square (□), circle (●) and cross (+) represent W1, W3, W10 and W13, respectively.

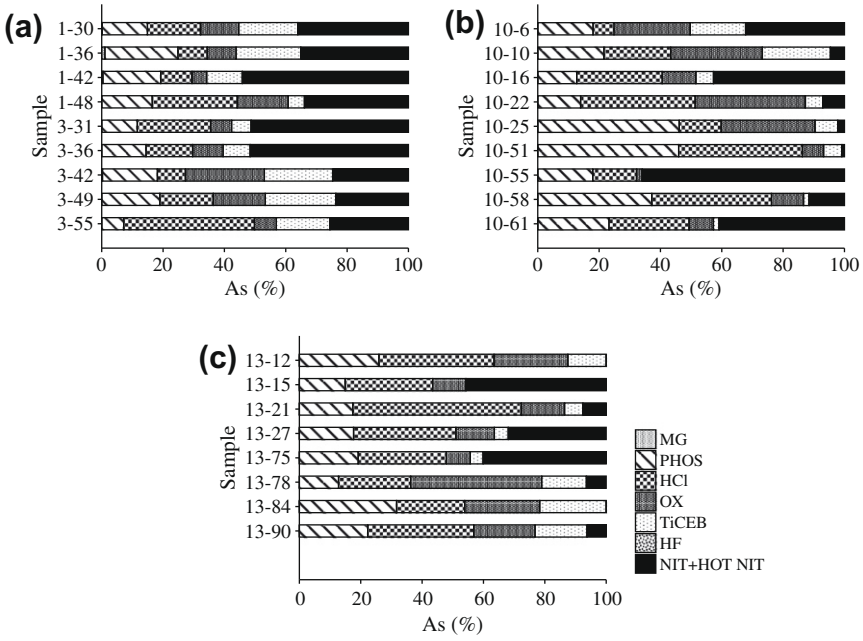


**Fig. 6.** Depth-variation profiles of As percentage among sequential extraction steps in (a) W1 and W3, (b) W10, and (c) W13.

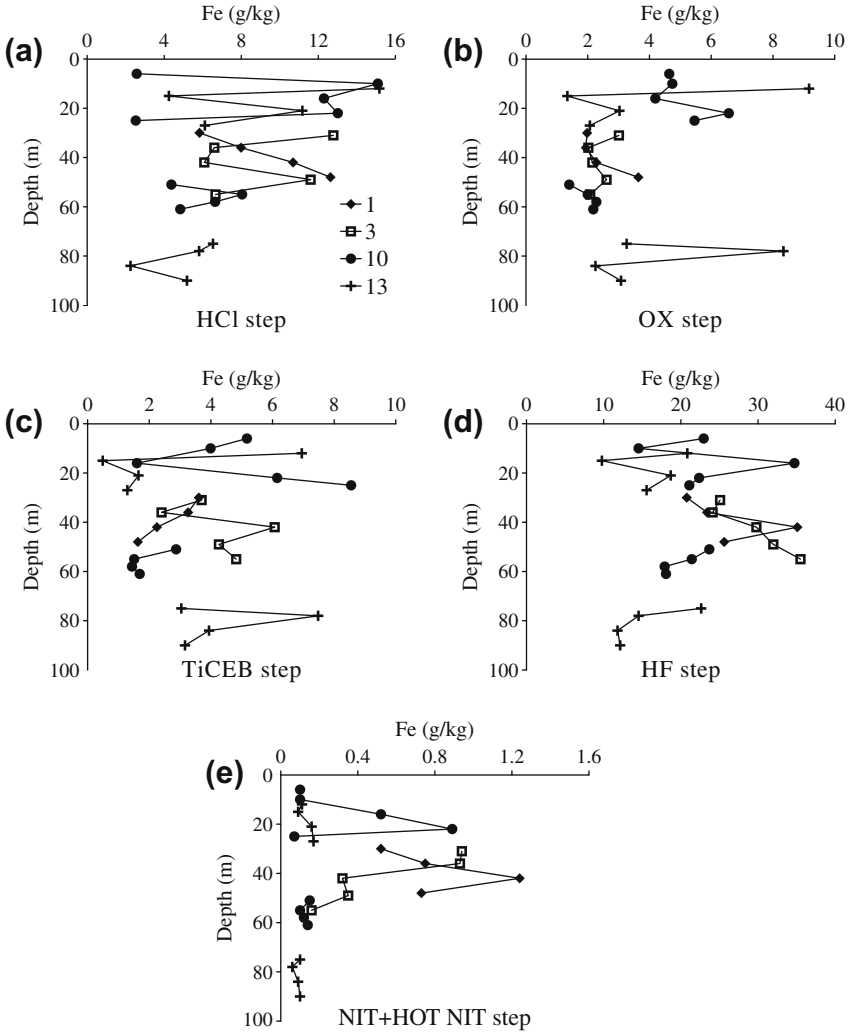


**Fig. 7.** Depth-variation profiles of Fe contents in the (a) HCl step, (b) OX step, (c) TiCEB step, (d) HF, and (e) NIT + HOT NIT step. Diamond (♦), hollow square (□), circle (●) and cross (+) represent W1, W3, W10 and W13, respectively.

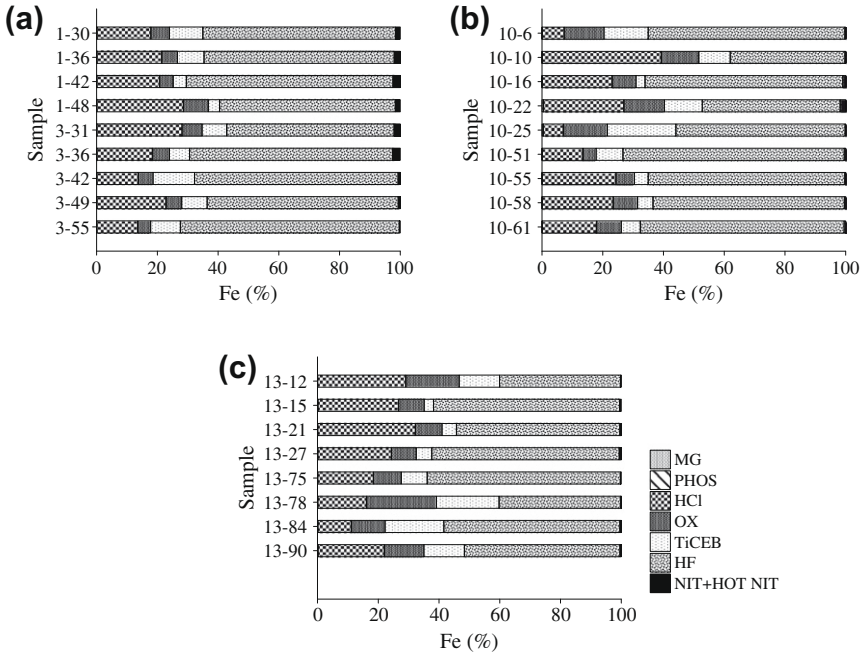


**Fig. 8.** Depth-variation profiles of Fe percentage among sequential extraction steps in (a) W1 and W3, (b) W10, and (c) W13.

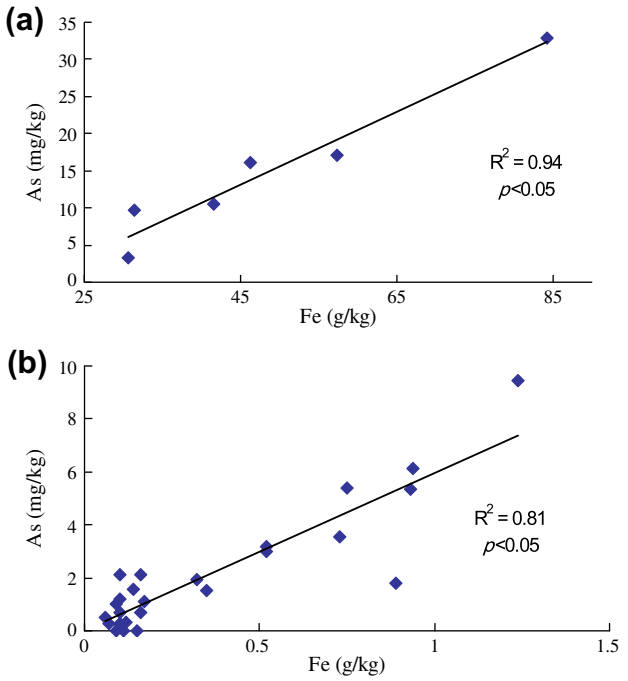


**Fig. 9.** (a) The correlation between cumulative As and Fe leached in the HCl, OX, and TiCEB extracts within the range of screen, and (b) the correlation between As and Fe in the NIT pool in all cores.

relations observed between As and $HCO_3^-$ ($r^2 = 0.84$, $p < 0.05$) and $PO_4^{3-}$ ($r^2 = 0.62$, $p < 0.05$) demonstrate that specific portions of As in the aqueous phase are related to ionic competition (Fig. 10a and e). Due to this competition there is poor correlation between aqueous As and Fe concentrations (Kim et al., 2000; Appelo et al., 2002). Hence, in this study the replacement reaction of ions such as $HCO_3^-$ and $PO_4^{3-}$ is likely to contribute to the release of As and is proposed as an explanation of the weak correlation between Fe and As concentrations in the anoxic groundwater system.

### *4.3. Effects of water table oscillation and ionic interaction on aqueous As and Fe concentrations*

Poor correlation between As and Fe concentrations in groundwater is explained in two possible ways. First, due to seasonal change (i.e., monsoon) and excessive pumping of groundwater for agriculture and aquaculture, the water table may oscillate concomitantly with the varying redox conditions beneath the surface. Meanwhile, intrusion of seawater followed by the introduction of $O_2$ also occurred. Hence, Fe concentrations, particularly Fe(II), in the groundwater may react with $O_2$ to precipitate as amorphous Fe(III) oxyhydroxides. According to the definition of sequential extracts by Keon et al. (2001), the HCl, OX and TiCEB extracts accounted for most of the Fe oxyhydroxides in the sediments. Competition by species such as $H_4SiO_4$, $HCO_3^-$, $H_2PO_4^-$ and $HPO_4^{2-}$ inhibit the precipitation of crystalline Fe(III) oxyhydroxide phases (Rose et al., 1996; Waychunas et al., 1996; Doelsch et al., 2000; Ma-

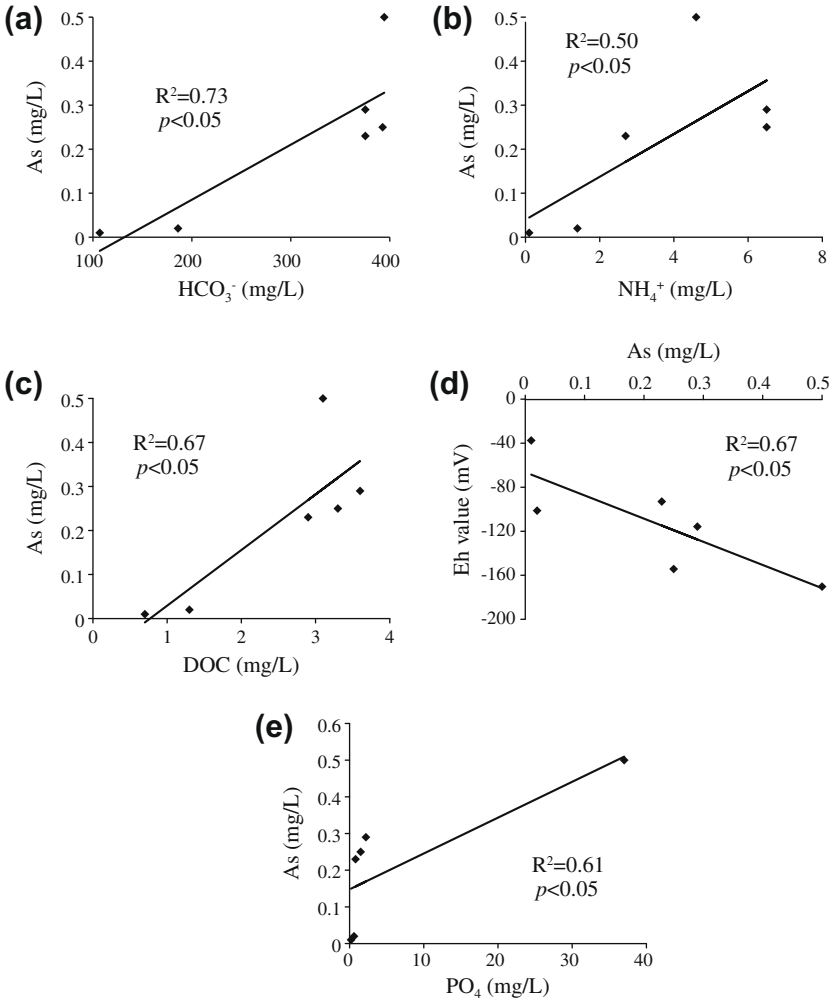


**Fig. 10.** Correlation of (a) $HCO_3^-$, (b) $NH_4^+$, (c) DOC, (d) $E_H$ value and (e) $PO_4$ with aqueous As concentration.

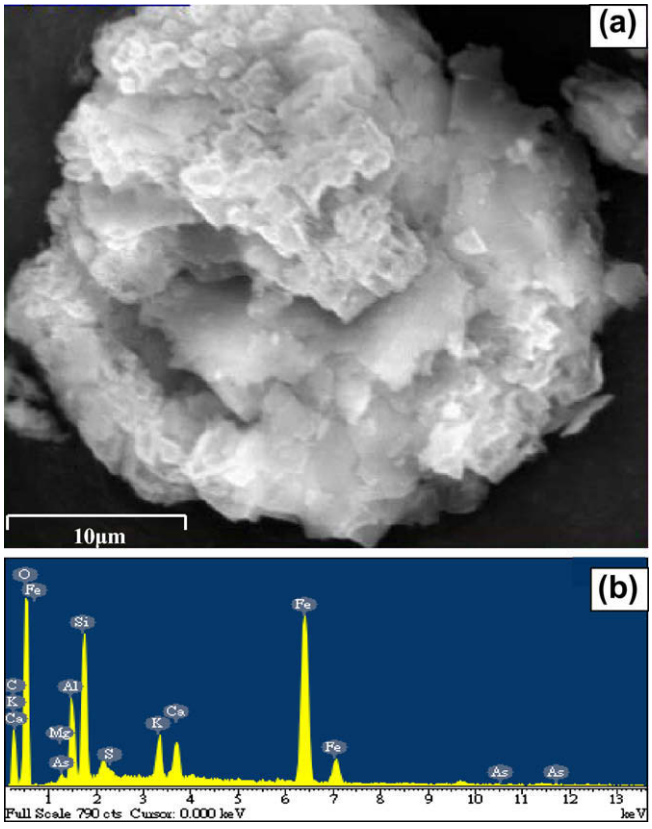


**Fig. 11.** Scanning electron microscope analysis of sample 1–48. (a) A mixed mineral of Fe, Si and Al carbonate and (b) EDS data.

sion et al., 2001). The Fe concentration in the HCl pools (i.e. the amorphous form of Fe oxyhydroxides) had a more complex distribution than those in the OX and TiCEB extracts within the well screen interval, indicating the combined effects of the exposure to $O_2$ and competitive ionic reactions, because of the fluctuation of the water table via either natural or anthropogenic activity.

Secondly, ionic reactions were responsible for inconsistent correlation between aqueous As and Fe concentrations. The main interactions between Fe and $HCO_3^-$, and $PO_4^{3-}$ were described above. In general, these reactions occurred along with the precipitations of siderite and vivianite (Appelo et al., 2002; Swartz et al., 2004). Although these precipitates were not identification, a mixed mineral of Fe, Si and Al carbonate was observed in this area (Fig. 11). Moreover, salinization was the main factor that was responsible for the local hydrochemistry and affected the initial composition of groundwater in the distal-fan (Wang et al., 2007). The increase in ionic strength of the groundwater could trigger the mobility of As (Keon et al., 2001). A conceptual diagram of the As cycle in the southern Choushui River alluvial fan, Taiwan is outlined here (Fig. 12). The Fe oxyhydroxides acted as the major sink of As in the oxidizing conditions and acted as a major source of As in the presence of reducing condition. The dual role of Fe oxyhydroxides governed As cycling in this area.

## 5. Conclusions

With the objective of identifying the geochemical conditions related to the sink/source of As in the subsurface, a comprehensive geochemical survey of the As-affected area of the southern Choushui River alluvial fan, Taiwan was conducted. Typically, local groundwater was characterized as low $E_H$ with low concentrations of $SO_4^{2-}$ and $NO_3^-$ accompanying high concentrations of $HCO_3^-$ and $NH_4^+$, confirming the reducing condition of subsurface aquifers. Aside from the good correlations observed between As and S, and Fe concentrations via the XRF data, sequential extraction results supported the association of As with Fe minerals and As-bearing sulfides, especially in the distal-fan, suggesting that the major sinks of As were associated with these minerals. The dual roles of Fe oxyhydroxides as the sink and source are governed by the local redox condition in the aquifer.

In addition, as interpreted from groundwater analyses, correlations between As and $HCO_3^-$, $NH_4^+$, TOC and $E_H$ values supported the hypothesis of reductive dissolution of Fe oxyhydroxides mediated by microbial activities. Competitive adsorption reactions of $HCO_3^-$

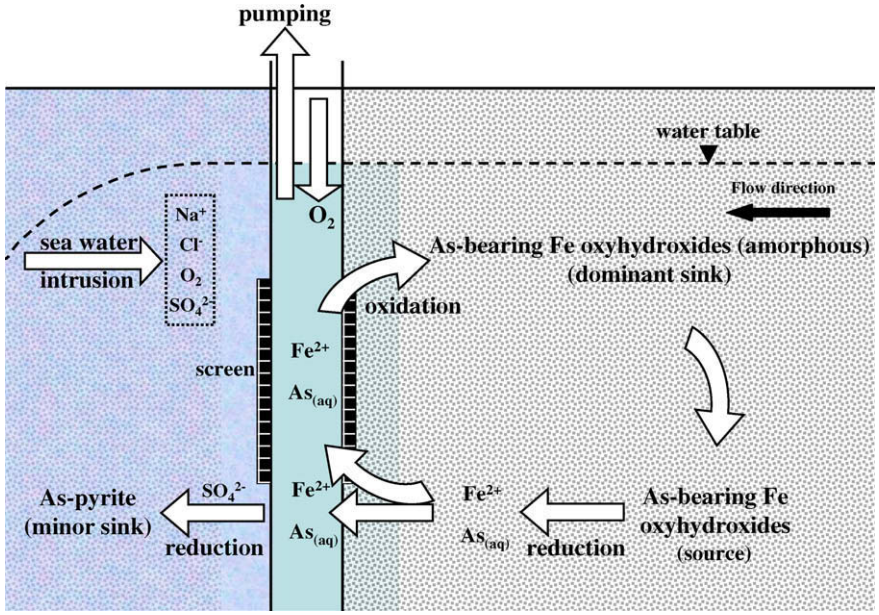


**Fig. 12.** Proposed As cycle in the sedimentary aquifers. Arsenic-bearing Fe oxyhydroxides are postulated to be the dominant sink under oxidizing conditions in the well screen area and acted as the dominant source in the reducing aquifer environment. Pyrite was also characterized as a minor sink of As under reducing conditions and is related with the supplement of $SO_4^{2-}$ via seawater intrusion.

and $PO_4^{3-}$ ions were also confirmed. Moreover, ionic competition causing mobility of As also explains the poor correlation between aqueous As and Fe concentrations in this area. Seasonal changes and excessive pumping along with redox cycling not only identified the heterogeneous distribution of Fe contents within the screen areas, but also contributed to the poor correlation between aqueous As and Fe concentration. However, biological conditions in this area need to be further explored to confirm that the reductive dissolution of Fe oxyhydroxides was driven by microbial degradation of organic matter.

## Acknowledgements

This work has been supported by the National Science Council of the Republic of China, Taiwan, under Contract No. NSC-93-2313-B-002-071. We thank Dr. Ron Fuge, Dr. David Polya and three anonymous reviewers for their constructive reviews. Ted Knoy is appreciated for his editorial assistance.

## References

Akai, J., Izumi, K., Fukuhara, H., Masuda, H., Nakano, S., Yoshimura, T., Ohfuji, H., Anawar, H.M., Akai, K., 2004. Mineralogical and geomicrobiological investigations on groundwater arsenic enrichment in Bangladesh. Appl. Geochem. 19, 215–230.

Anawar, H.M., Akai, J., Komaki, K., Terao, H., Yoshioka, T., Ishizuka, T., Safiullah, S., Kato, K., 2003. Geochemical occurrence of arsenic in groundwater of Bangladesh: sources and mobilization processes. J. Geochem. Explor. 77, 109–131.

APHA, 1998. Standard Methods for the Examination of Water and Waste Water, twentieth ed. American Public Health Assoc, Washington, DC. pp. 413–426.

Appelo, C.A.J., Van der Weiden, M.J.J., Tournassat, C., Charlet, L., 2002. Surface complexation of ferrous iron and carbonate on ferrihydrite and the mobilization of arsenic. Environ. Sci. Technol. 36, 3096–3103.

Banfield, J.F., Nealson, K.H., Lovley, D.R., 1998. Geomicrobiology: interactions between microbes and minerals. Science 280, 54–55.

BGS/DPHE, 2001. Arsenic contamination of groundwater in Bangladesh. In: Kinniburgh, D.G., Smedley, P.L. (Eds.), BGS Technical Report WC/00/19, British Geological Survey, Keyworth, UK.

Bhattacharya, P., Jacks, G., Ahmed, K.M., Khan, A.A., Routh, J., 2002. Arsenic in groundwater of the Bengal delta plain aquifers in Bangladesh. Bull. Environ. Contam. Toxicol. 69, 538–545.

Bhattacharya, P., Welch, A.H., Stollenwerk, K.G., McLaughlin, M.J., Bundschuh, J., Panaullah, G., 2007. Arsenic in the environment: biology and chemistry. Sci. Total Environ. 379, 109–120.

Central Geological Survey, 1999. Project of Groundwater Monitoring Network in Taiwan during First Stage-Research Report of Chou-Shui River Alluvial Fan. Taiwan, Water Resources Bureau.

Chapelle, F.H., 2000. The significance of microbial processes in hydrogeology and geochemistry. Hydrogeol. J. 8, 41–46.

Chapelle, F.H., Lovley, D.R., 1992. Competitive exclusion of sulfate reduction by Fe(III)-reducing bacteria: a mechanism for producing discrete zones of high-iron groundwater. Ground Water 30, 29–36.

Chen, W.F., Liu, T.K., 2003. Dissolved oxygen and nitrate of groundwater in Choushui Fan-Delta, western Taiwan. Environ. Geol. 44, 731–737.

Chen, C.J., Dzeng, S.R., Yang, M.H., Chiu, K.H., Shieh, G.M., Wai, C.M., 1994. Arsenic species in groundwaters of the blackfoot disease area, Taiwan. Environ. Sci. Technol. 28, 877–881.

Doelsch, E., Rose, J., Masion, A., Bottero, J.-Y., Nahon, D., Bertsch, P.M., 2000. Speciation and crystal chemistry of Fe(III) chloride hydrolyzed in the presence of $SiO_4$ ligands. 1: an Fe K-edge EXFAS study. Langmuir 16, 4726–4731.

Guo, H.R., Chen, C.J., Greene, H.L., 1994. Arsenic in drinking water and cancers: a brief descriptive view of Taiwan studies. In: Chappell, W.R., Abernathy, C.O., Cothern, C.R. (Eds.), Arsenic Exposure and Health. Science and Technology Letters, Northwood, pp. 129–138.

Harvey, C.F., Swartz, C.H., Badruzzaman, A.B.M., Keon-Blute, N., Niedan, V., Brabander, D., Oates, P.M., Ashfaque, K.N., Islam, S., Hemond, H.F., Ahmed, M.F., 2002. Arsenic mobility and groundwater extraction in Bangladesh. Science 298, 1602–1606.

Hossain, M.F., 2006. Arsenic contamination in Bangladesh – an overview. Agric. Ecosyst. Environ. 113, 1–16.

Islam, F.S., Pederick, R.L., Gault, A.G., Adams, L.K., Polya, D.A., Charnock, J.M., Lloyd, J.R., 2005. Interactions between the Fe(III)-reducing bacterium Geobacter sulfurreducens and arsenate, and capture of the metalloid by biogenic Fe(II). Appl. Environ. Microbiol. 71, 8642–8648.

Keon, N.E., Swartz, C.H., Brabander, D.J., Harvey, C., Hemond, H.F., 2001. Validation of an arsenic sequential extraction method for evaluating mobility in sediments. Environ. Sci. Technol. 35, 2778–2784.

Kim, M.J., Nriagu, J., Haack, S., 2000. Carbonate ions and arsenic dissolution by groundwater. Environ. Sci. Technol. 34, 3094–3100.

Klein, C., Hurlbut Jr., C.S., 1999. Oxides, Hydroxides, and Halides. Manual of Mineralogy, 21st ed. John Wiley & Sons, New York. pp. 372–402, Chapter 11.

Kocar, B.D., Herbel, M.J., Tufano, K.J., Fendorf, S., 2006. Contrasting effects if dissimilatory iron(III) and arsenic(V) reduction on arsenic retention and transport. Environ. Sci. Technol. 40, 6715–6721.

Kocar, B.D., Polizzotto, M.L., Benner, S.G., Ying, S.C., Ung, M., Ouch, K., Samreth, S., Suy, Bunseang., Phan, K., Sampson, M., Fendorf, S., 2008. Integrated biogeochemical and hydrologic processes driving arsenic release from shallow sediments to groundwaters of Mekong delta. Appl. Geochem. 23, 3059–3071.

Lenoble, V., Bouras, O., Deluchat, V., Serpaud, B., Bollinger, J.C., 2002. Arsenic adsorption onto pillared clays and iron oxides. J. Colloid Interface Sci. 255, 52–58.

Liu, C.W., 1999. Compilation 'Groundwater in Taiwan-Choushuichi Alluvial Plain'. Taiwan, Water Resources Bureau.

Liu, C.W., Lin, K.H., Kuo, Y.M., 2003. Application of factor analysis in the assessment of groundwater quality in a blackfoot disease area in Taiwan. Sci. Total Environ. 313, 77–89.

Liu, C.W., Wang, S.W., Jang, C.S., Lin, K.H., 2006. Occurrence of arsenic in ground water in the Choushui River alluvial fan, Taiwan. J. Environ. Qual. 35, 68–75.

Lovley, D.R., 1997. Microbial Fe(III) reduction in subsurface environments. FEMS Microbiol. Rev. 30, 305–313.

Masion, A., Rose, J., Bottero, J.Y., Tchoubar, D., Elmerich, P., 2001. Speciation and crystal chemistry of Iron(III) chloride hydrolyzed in the presence of $SiO_4$ ligands. 3. Semilocal scale structure of the aggregates. Langmuir 17, 4753–4757.

McArthur, J.M., Ravenscroft, P., Safiulla, S., Thirlwall, M.F., 2001. Arsenic in groundwater: testing pollution mechanisms for sedimentary aquifers in Bangladesh. Water Resour. Res. 37, 109–117.

McArthur, J.M., Banerjee, D.M., Hudson-Edwards, K.A., Mishra, R., Purohit, R., Ravenscroft, P., Cronin, A., Howarth, R.J., Chatterjee, A., Talukder, T., Lowry, D., Houghton, S., Chadha, D.K., 2004. Natural organic matter in sedimentary basins and its relation to arsenic in anoxic ground water: the example of West Bengal and its worldwide implications. Appl. Geochem. 19, 1255–1293.

Nealson, K.H., 1997. Sediment bacteria: who's there, what are they doing, and what's new? Ann. Rev. Earth Planet. Sci. 25, 403–434.

Nickson, R.T., McArthur, J.M., Burgess, W.G., Ahmed, K.M., Ravenscroft, P., Rahman, M., 1998. Arsenic poisoning of Bangladesh groundwater. Nature 395, 338.

Nickson, R.T., McArthur, J.M., Ravenscroft, P., Burgess, W.G., Ahmed, K.M., 2000. Mechanism of arsenic release to groundwater, Bangladesh and West Bengal. Appl. Geochem. 15, 403–413.

Nickson, R.T., McArthur, J.M., Shrestha, B., Kyaw-Myint, T.O., Lowry, D., 2005. Arsenic and other drinking water quality issues, Muzaffargarh district, Pakistan. Appl. Geochem. 20, 55–68.

Rose, J., Manceau, A., Bottero, J.–Y., Masion, A., Garcia, F., 1996. Nucleation and growth mechanisms of Fe oxyhydroxide in the presence of $PO_4$ ions. 1. Fe K-edge EXAFS. Langmuir 12, 6701–6707.

Rowland, H.A.L., Gault, A.G., Lythgoe, P., Polya, D.A., 2008. Geochemistry of aquifer sediments and arsenic-rich groundwaters from Kandal Province, Cambodia. Appl. Geochem. 23, 3029–3046.

Sherman, D.M., Randall, S.R., 2003. Surface complexation of arsenate(V) to iron(III) (hydr)oxides: structural mechanism from ab initio molecular geometries and EXAFS spectroscopy. Geochim. Cosmochim. Acta 67, 4223–4230.

Shimada, N., 1996. Geochemical conditions enhancing the solubilization of arsenic into groundwater in Japan. Appl. Organometal. Chem. 10, 667–674.

Smedley, P.L., Kinniburgh, D.G., 2002. A review of the source, behaviour and distribution of arsenic in natural waters. Appl. Geochem. 17, 517–568.

Stollenwerk, K.G., Breit, G.N., Welch, A.H., Yount, J.C., Whitney, J.W., Foster, A.L., Uddin, M.N., Majumder, R.K., Ahmed, N., 2007. Arsenic attenuation by oxidized aquifer sediments in Bangladesh. Sci. Total Environ. 379, 133–150.

Swartz, C.H., Blute, N.K., Badruzzman, B., Ali, A., Brabander, D., Jay, J., Besancon, J., Islam, S., Hemond, H.F., Harvey, C.F., 2004. Mobility of arsenic in a Bangladesh aquifer: Inferences from geochemical profiles, leaching data, and mineralogical characterization. Geochim. Cosmochim. Acta 68, 4539–4557.

Taiwan Sugar Company, 1999. Establishment and Operational Management of Groundwater Monitoring Network. Taiwan, Water Resource Bureau.

Taiwan Sugar Company, 2000. Groundwater Quality Survey and Analysis of Groundwater Monitoring Network (2/5). Taiwan, Water Resource Bureau.

Taiwan Sugar Company, 2003. Groundwater Quality Survey and Analysis of Groundwater Monitoring Network (5/5). Taiwan, Water Resource Bureau.

Taiwan Sugar Company, 2006. Analysis and Evaluation of the Groundwater Quality Survey in Taiwan Area. Taiwan, Water Resource Bureau.

Tseng, W.P., 1977. Effects and dose–response relationships of skin cancer and blackfoot disease with arsenic. Environ. Health Perspect. 19, 109–119.

USEPA, 1997. Acid Digestion of Sediments, Sludges and Soils. EPA 3050b, USEPA, Athens, GA. (<http://www.epa.gov>).

Wang, S.W., Liu, C.W., Jang, C.S., 2007. Factors responsible for high arsenic concentrations in two groundwater catchments in Taiwan. Appl. Geochem. 22, 460–467.

Waychunas, G.A., Fuller, C.C., Rhea, B.E., Davis, J.A., 1996. Wide angle X-ray scattering (WAXS) study of "two-line" ferrihydrite structure: effect of arsenate adsorption and counterion variation and comparison with EXAFS results. Geochim. Cosmochim. Acta 10, 1765–1781.

Zheng, Y., Stute, M., van Geen, A., Gavrieli, I., Dhar, R., Simpson, H.J., Schlosser, P., Ahmed, K.M., 2004. Redox control of arsenic mobilization in Bangladesh groundwater. Appl. Geochem. 19, 201–214.